Subaortic Cavitated Myxoma Causing Severe Left Ventricular Outflow Tract Obstruction in a Young Dog

Jonathan P. Stack, DVM, MS, Ryan C. Fries, DVM, DACVIM (Cardiology), and
Jonathan P. Samuelson, DVM, MS, DACVP, *Urbana, Illinois*

INTRODUCTION

Cardiac myxoma is a relatively rare neoplasm reported in the veterinary literature.[1-9] A single case of a large myxoma causing a left ventricular outflow tract obstruction (LVOTO) has been reported in a 12-year-old dog that died suddenly.[4] Here we present a case of a myxoma with an atypical cavitated morphology causing an LVOTO in a 1-year-old dog that was initially misdiagnosed as an atypical presentation of congenital subaortic stenosis.

CASE PRESENTATION

A 1-year-old, intact female mixed-breed dog was presented to the cardiology service for evaluation of a grade VI/VI left basilar systolic murmur and weak femoral pulses bilaterally.

Two-dimensional (2D) and M-mode transthoracic echocardiography (TTE) found moderate left ventricular (LV) concentric hypertrophy and mild left atrial (LA) enlargement. A thin-walled structure with a cavitated appearance was present on the basilar interventricular septum of the left ventricle proximal to the aortic valve (Figure 1). The size of the structure changed dynamically, appearing to expand during systole and collapsing during diastole. On color Doppler imaging, turbulent flow, based on aliasing, could be detected at the level of the cavitated structure (Video 1). Spectral Doppler interrogation of the LV outflow tract (LVOT) showed severely elevated peak LVOT systolic velocity (6.69 m/sec). Other findings included subjective mild thickening of the mitral valve leaflets and moderate mitral regurgitation. Three-dimensional (3D) TTE was performed, which provided further evidence of a cavitated structure in the LVOT (Figure 2). A simultaneous electrocardiogram (ECG) during the echocardiographic studies showed a sinus rhythm.

Due to the reported age of the patient, the cavitated structure was initially suspected to be a congenital anomaly resulting in an unusual manifestation of subaortic stenosis. The patient was prescribed carvedilol (0.82 mg/kg) orally every 12 hours. Given the severity of the obstruction and evidence of LV and LA remodeling, balloon dilation of the LVOT was discussed as a potential palliative treatment option.

The patient was reevaluated approximately 10 weeks later for possible balloon dilation. No signs of exercise intolerance, syncope, or other abnormalities were reported. Physical examination revealed a new irregular heart rhythm with pulse deficits. A recheck echocardiogram with simultaneous ECG found no significant progression in LV or LA dimensions; however, there was no improvement in LVOT systolic velocity (7.19 m/sec) with beta blocker therapy. The ECG showed an underlying sinus rhythm with frequent, single ventricular premature complexes of right bundle branch block morphology in lead II, suggestive of left-sided origin. With this new finding, the patient was prescribed sotalol (2.5 mg/kg) orally every 12 hours and the carvedilol was discontinued. Cross-sectional imaging and a combination cutting balloon followed by a high-pressure balloon valvuloplasty procedure was planned for the following day using a previously published protocol for subaortic stenosis in dogs as a guideline.[10]

Prior to balloon dilation, the anesthetized patient underwent cardiac-gated magnetic resonance imaging (CMR) for further evaluation of the cavitated structure and myocardium. The CMR study was performed on a MAGNETOM Skyra 3T scanner with an 18-channel phased-array body coil and software version syngo MR E11 (Siemens Healthcare, Erlangen, German). Cine-images were acquired using a balanced steady-state precession (bSSFP) sequence in combination with parallel imaging and retrospective gating. Left ventricular systolic function and morphology imaging was accomplished utilizing bSSFP scanning with whole-heart coverage (aortic root to LV apex) of gapless short-axis slices, with retrospective gating and multiple end-expiratory breath holds. T1 mapping was performed using a modified Look-locker inversion recovery sequence from a short-axis plane at the base, middle, and apical LV chamber using a single–breath hold, ECG-triggered sequence. The T1 maps were acquired before and 15 minutes after contrast injection of 0.2 mL/kg (0.1 mmol/kg) gadopentetate dimeglumine (Magnevist; Bayer Healthcare, Wane, NJ). Late gadolinium enhancement images were obtained 10 minutes after the bolus of gadopentetate dimeglumine using an inversion-recovery gradient echo technique. Velocity-encoded, through-plane imaging was employed to measure flow volumes throughout the cardiac cycle at selected locations within the descending aorta and LVOT. There was increased myocardial mass (136.1 g) based on left ventricle–to–body weight ratios = .86 (normal = .43 ± 0.08). T1 mapping indicated increased myocardial interstitial fibrosis based on native T1 time (1,130 msec) and increased extracellular volume

VIDEO HIGHLIGHTS

Video 1: TTE 2D and color Doppler imaging from the right parasternal long-axis view. A cavitated structure (*red arrow*) is present on the septal surface of the LVOT, proximal to the aortic valve leaflets. The cavitated structure is dynamic and changes in size throughout the cardiac cycle. Color Doppler indicates aliasing blood flow around the cavitated structure as well as trace aortic insufficiency.

Video 2: Cardiac magnetic resonance imaging. Three-chamber view steady-state free precession cine-image showing cavitated structure (*red arrow*) arising from the interventricular septum, moderate LV concentric hypertrophy, and aliasing blood flow in the LVOT and ascending aorta during systole. The cavitated structure is dynamic in size, is largest during end systole, and communicates with the blood pool.

Video 3: TEE 2D, color Doppler, and 3D imaging of the LVOT. A cavitated structure is present in the LVOT (*red arrow*) creating a dynamic subvalvular obstruction. Color Doppler indicates aliasing blood flow around the cavitated structure as well as mild aortic insufficiency. Three-dimensional imaging reveals the dynamic change in size of the cavitated structure throughout the cardiac cycle.

View the video content online at www.cvcasejournal.com.

---

fraction (28.1%). There was no evidence of late gadolinium enhancement, and velocity-encoded through-plane imaging indicated severely increased LVOT systolic velocity (LVOT velocity = 4.86 m/sec, 94.5 mm Hg) with mildly reduced stroke volume (21.3 mL) and car-diac output (1.98 L/minute). Short- and long-axis cine-imaging of the LV outflow identified a cavitated mass-like structure obstructing the LV outflow in a dynamic fashion during middle and end systole (Video 2). The mass was hollow and communicated directly with the blood pool. There was no direct communication with the coronary artery, the anterior mitral valve leaflet, or the aortic valve leaflets, which ruled out an ectopic coronary artery or atypical valvular dysplasia causing LVOTO.[11,12]

Immediately following CMR, the patient underwent a balloon dilation procedure. Throughout the procedure, 2D and 3D transesophageal echocardiography (TEE) was performed. High-quality images of the LVOT were obtained before balloon valvuloplasty to allow comparison with postvalvuloplasty imaging (Figure 3 and Video 3).

The surgical approach was made via a carotid artery cut down in left lateral recumbency as previously described in dogs.[10] Direct LV pressures, measured using a 5 Fr pigtail catheter, were 117 mm Hg systolic and 7 mm Hg diastolic, with a mean pressure of 43 mm Hg. Iohexol solution was injected into the LV lumen, and flow through the LVOT and aorta was observed. The cavitated structure could be seen filling with contrast agent during systole and collapsing during diastole, consistent with what had been previously observed on echocardiography and CMR. A cutting balloon valvuloplasty was performed under fluoroscopic guidance. Utilizing TEE, inflation of the 7 mm × 20 mm cutting balloon allowed it to visibly engage with the cavitated structure within the LVOT. Inflation of the cutting balloon was performed two additional times, with slight repositioning of the balloon prior to each inflation to allow the atherotomes to engage with additional sites in the LVOT. The cutting balloon was withdrawn, and a 12 mm × 60 mm high-pressure balloon valvuloplasty was performed. Balloon–to–aortic annulus ratios were as follows: 1.07 for 2D TTE, 0.98 for 3D TEE, 1.01 for CMR, and 0.94 for angiography. The balloon was inflated to 10 atm, with an inflation device, a total of three times. Three-dimensional TEE evaluation of the lesion after three inflations showed no obvious change
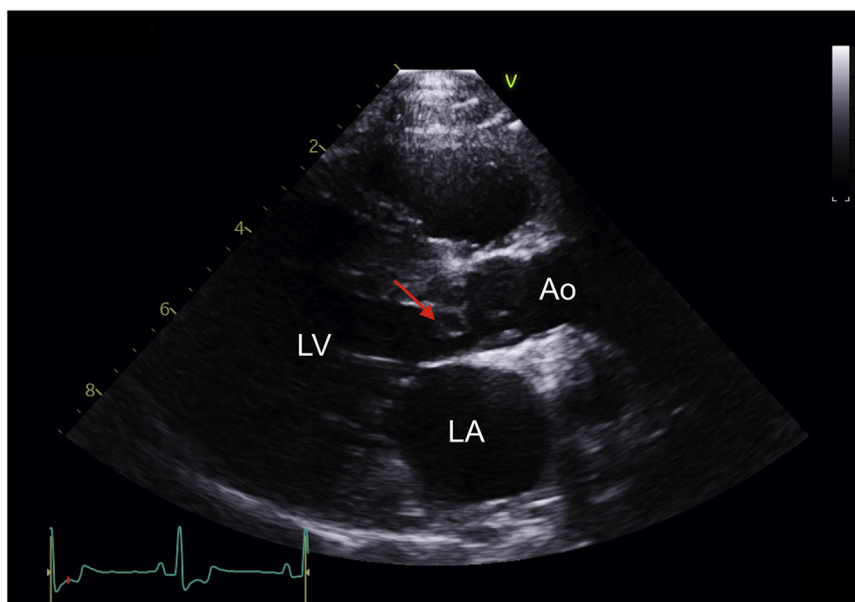

Figure 1 TTE 2D imaging from the right parasternal long-axis view. A cavitated structure (*red arrow*) is present on the septal surface of the LVOT, proximal to the aortic valve leaflets. *Ao*, Aorta; *LA*, left atrium; *LV*, left ventricle.
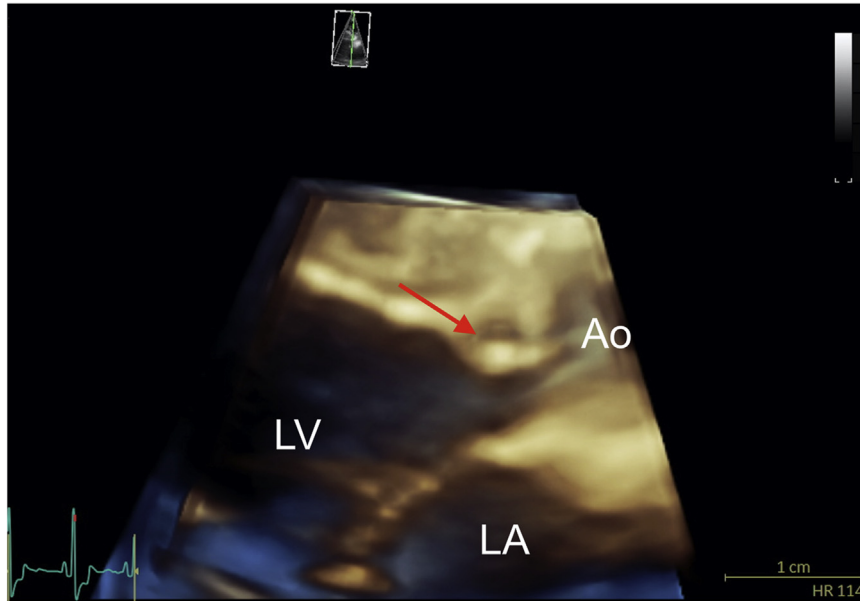
Figure 2 TTE 3D imaging from the right parasternal long-axis view. A cavitated structure (*red arrow*) is present on the septal surface of the LVOT, proximal to the aortic valve leaflets. *Ao*, Aorta; *LA*, left atrium; *LV*, left ventricle.
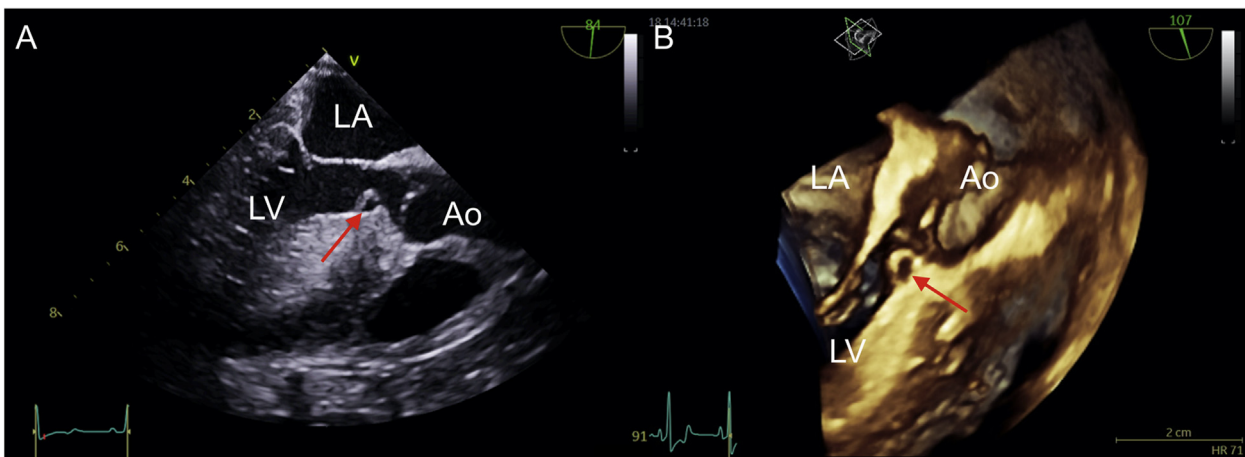

Figure 3 TEE 2D **(A)** and 3D **(B)** imaging of the LVOT was performed to guide combined cutting and high-pressure balloon valvuloplasty. A cavitated structure (*red arrow*) is present along the septal surface of the LVOT. *Ao*, Aorta; *LA*, left atrium; *LV*, left ventricle.

with continued dynamic expansion and collapse of the structure corresponding with systole and diastole, respectively.

A repeat 2D TTE performed the next day showed no obvious changes to the cavitated structure, and spectral Doppler measurement of LVOT velocity was 6.85 m/sec. The patient was discharged and scheduled for reevaluation in 1 month. Four days prior to her recheck evaluation the patient experienced a presyncopal episode during a leash walk. Approximately 2 minutes after the event, the patient collapsed into sternal recumbency and appeared dazed but recovered in approximately 5 minutes. A recheck echocardiogram was performed, which showed an LVOT systolic velocity of 6.49 m/sec. A 24-hour ambulatory ECG monitor was also placed at this visit. An underlying sinus rhythm was noted with no evidence of ventricular or atrial ectopy or significant pauses. An episode was not observed during the Holter period; however, given the absence of any arrhythmias, no changes were made to the medications, and the episode was presumed to be secondary to the severe LVOTO.

Approximately 7 months later, additional episodes that resembled presyncopal events were noted. The patient did not collapse during these episodes and appeared weak and pale. A recheck echocardiogram was performed, which showed persistence of the severe LVOTO but no evidence of significant progression of LV or LA remodeling. A concurrent ECG (lead II) at the time showed a sinus rhythm. Following the echocardiogram, the patient was placed in a kennel while waiting to be discharged. Approximately 2 hours after the echocardiogram, the patient was walked outside, acutely collapsed, and was found to be in ventricular tachycardia with a rate of 250 beats per minute. A 2 mg/kg bolus of lidocaine was administered

Figure 4 Subgross photomicrograph of the left ventricle (V), myxoma (M), aortic valve leaflet (L), and aorta (A). The myxoma is arising from the ventricular endocardial surface and occluding the LVOT. Hematoxylin and eosin stain, 0.37× magnification.

intravenously, and the rhythm progressed to ventricular fibrillation. Cardiopulmonary resuscitation efforts were initiated, including external defibrillation. Continued resuscitation efforts failed to reestablish sinus rhythm, and intracardiac pentobarbital sodium (2,340 mg) was administered to provide humane euthanasia at the owner's request.

On postmortem examination of the heart and great vessels, a 10.0 mm × 10.0 mm × 7.0 mm, white, firm mass was identified arising from the endocardial surface of the interventricular septum just ventral to the aortic valve leaflets, protruding into the lumen and obstructing the LVOT. The ventral aspect of the mass was detached from the endocardial surface, and there was a 5.0 mm × 5.0 mm × 3.0 mm central cavitation of the mass, consistent with what was observed on 2D and 3D TTE and TEE. Heart and aorta tissue specimens were then placed in 10% neutral-buffered formalin. Sections of the heart mass and aorta were submitted for routine histologic processing including hematoxylin and eosin staining (Figure 4). Microscopically, the mass was composed of stellate to spindloid neoplastic cells with moderate eosinophilic cytoplasm, an oval to elongate heterochromatic nucleus, and an indistinct nucleolus. Neoplastic cells were suspended in abundant pale eosinophilic wispy myxoid stroma. Anisocytosis and anisokaryosis were moderate, and no mitoses were identified in 10 high-power (400×) fields. No other histologic abnormalities were identified in the sections.

Additional histochemical and immunohistochemical staining was performed to further characterize the neoplasm. Neoplastic cells showed strong cytoplasmic reactivity to vimentin (Biocare Medical, LLC, mouse monoclonal, IgG1/kappa, V9 predilute antibody) immunohistochemical staining. Wispy eosinophilic stroma between neoplastic cells was strongly positive with Alcian-blue staining and negative to weakly positive with periodic acid-Schiff staining, consistent with mesenchymal-derived mucinous matrix. Gross and microscopic findings were consistent with myxoma arising from the LV endocardium (Figure 5).

DISCUSSION

Cardiac myxomas are rare in dogs, with only sporadic case reports present in the veterinary literature.[1-9] This is in contrast to humans, where myxomas are the most commonly identified primary cardiac tumor, with the most common location being within the left atrium.[13] In dogs, the majority of cases describe myxomas as affecting the right side of the heart, including the right atrium, tricuspid valve, and right ventricular outflow tract.[1,2,5,7-9] There have been three other case reports of myxoma on the left side of the heart in dogs: one in which an LA myxoma was identified in a dog with multiple masses resembling Carney complex; another that involved the mitral valve apparatus including the posterior papillary muscle, the chordae tendineae, and mitral valve leaflets, resulting in a secondary mitral stenosis; and a third report that also arose from the LVOT, causing a near-complete obstruction.[3,4,6] All of these myxomas involved large, solid masses. To our knowledge, our case report is unique both for the age of the patient (1 year old) as well as for the unusual, cavitated morphology of the mass causing a dynamic expansion and collapse of the mass corresponding with systole and diastole. Although pediatric myxomas have been reported in humans, to our knowledge, the youngest reported dog with a myxoma was 4 years old.[6] The unusually young presentation and appearance of the mass led to an initial misdiagnosis of an atypical form of severe congenital subaortic stenosis as well as an attempted balloon valvuloplasty.

Combination cutting and high-pressure balloons have been used to reduce pressure gradients and palliate clinical signs in dogs with severe subaortic stenosis.[14] The procedure in this patient failed to improve the severe LVOTO caused by the myxoma. On gross examination, the mass was found to be extremely firm, which may have made it resistant to scoring with the atherotomes of the cutting balloon or more resistant to tearing in the face of a high-pressure balloon. Additionally, the dynamic nature of the myxoma may have allowed for flattening of the surface and obliteration of the tumor cavity, further resisting cutting and tearing forces. The cause of the patient's
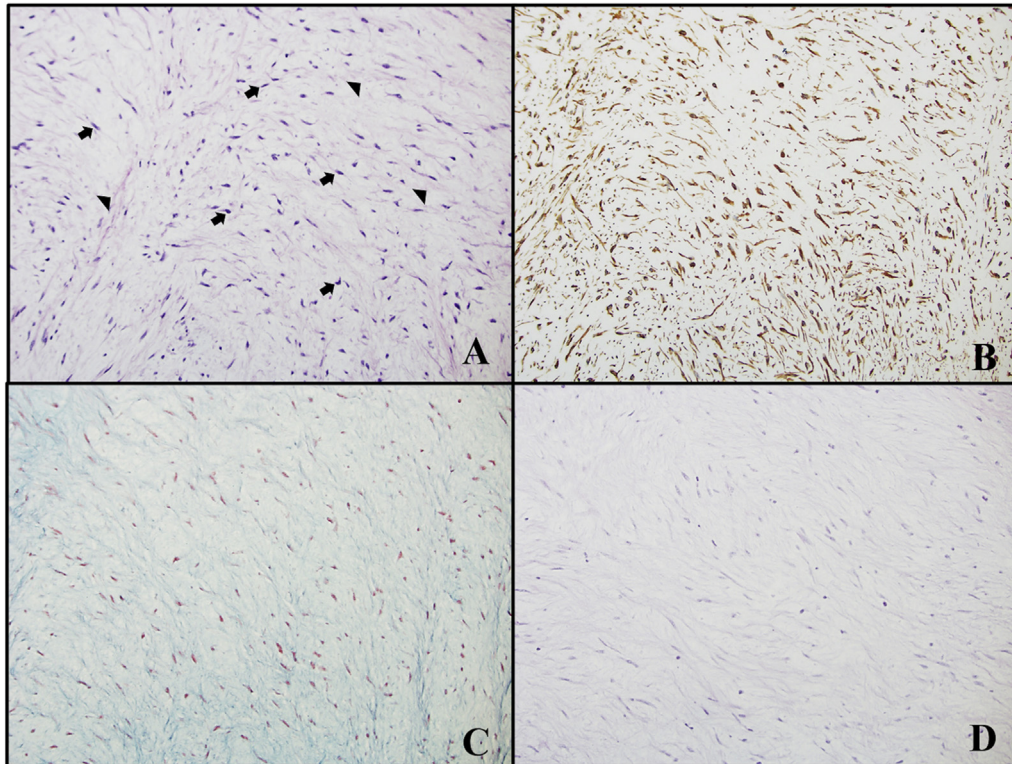
Figure 5 Photomicrographs of the myxoma. All images are 200× magnification. **(A)** The myxoma is composed of stellate to spindloid cells (*arrows*) in abundant myoid matrix (*arrowheads*). Hematoxylin and eosin stain. **(B)** Neoplastic cells stain positively (*brown*) for vimentin immunohistochemistry. **(C)** Myxoid matrix stains positive (*blue*) with Alcian-blue staining. **(D)** Myxoid matrix has little to no positive staining (expected to be bright pink) with periodic acid-Schiff staining.

repeated syncopal episodes remains unclear; however, it is possible that the events may have been induced by the severe LVOTO or may have been manifestations of paroxysmal ventricular tachycardia that was not identified on ambulatory ECG recordings. Although the patient had ventricular arrhythmias documented previously, these had appeared to be well controlled on sotalol. Sudden cardiac death is a known complication of severe subaortic stenosis in dogs and in humans. Pressure-induced hypertrophy, as seen in this dog, is thought to lead to myocardial ischemia, fibrosis, and reduced coronary reserve, which may precipitate the formation of lethal arrhythmias. Cardiac-gated magnetic resonance imaging results in this patient showed evidence of interstitial fibrosis; however, the impact of the other factors is not known in this patient.

CONCLUSION

Cardiac myxomas are rare cardiac tumors in dogs; however, our report shows that these should be considered as a possible differential diagnosis in identification of masses or unusual structures on the left side of the heart, even in young dogs. Our report also demonstrates the potential value of advanced imaging techniques such as CMR and 3D echocardiographic techniques in the further characterization of cardiac anomalies and pathologic changes. Increased usage of these modalities in veterinary medicine may improve interventional approaches as well as provide important prognostic information.

SUPPLEMENTARY DATA

Supplementary data to this article can be found online at https://doi.org/10.1016/j.case.2021.07.002.

REFERENCES

1. Darke PG, Gordon LR. Cardiac myxoma in a dog. Vet Rec 1974;95:565-7.
2. Machida N, Hoshi K, Kobayashi M, Katsuda S, Yamane Y. Cardiac myxoma of the tricuspid valve in a dog. J Comp Pathol 2003;129:320-4.
3. Adissu HA, Hayes G, Wood GA, Caswell JL. Cardiac myxosarcoma with adrenal adenoma and pituitary hyperplasia resembling Carney complex in a dog. Vet Pathol 2010;47:354-7.
4. de Nijs MI, Vink A, Bergmann W, Szatmári V. Left ventricular cardiac myxoma and sudden death in a dog. Acta Vet Scand 2016;58:41.
5. Akkoc A, Ozyigit MO, Cangul IT. Valvular cardiac myxoma in a dog. J Vet Med A Physiol Pathol Clin Med 2007;54:356-8.
6. Fernandez-del Palacio MJ, Sanchez J, Talavera J, Martínez C. Left ventricular inflow tract obstruction secondary to a myxoma in a dog. J Am Anim Hosp Assoc 2011;47:217-23.

7. Roberts SR. Myxoma of the heart in a dog. J Am Vet Med Assoc 1959;134: 185-8.

8. Briggs OM, Kirberger RM, Goldberg NB. Right atrial myxosarcoma in a dog. J S Afr Vet Assoc 1997;68:144-6.

9. Bright JM, Toal RL, Blackford LA. Right ventricular outflow obstruction caused by primary cardiac neoplasia. Clinical features in two dogs. J Vet Intern Med 1990;4:12-6.

10. Kleman ME, Estrada AH, Maisenbacher HW, Prošek R, Pogue B, Shih A, et al. How to perform combined cutting balloon and high pressure balloon valvuloplasty for dogs with subaortic stenosis. J Veterinary Cardiol 2012; 14:351-61.

11. Otoni C, Abbott JA. Mitral valve dysplasia characterized by isolated cleft of the anterior leaflet resulting in fixed left ventricular outflow tract obstruction. J Vet Cardiol 2012;14:301-5.

12. Pirelli L, Yu P-J, Srichai MB, Khvilivitzky K, Angelini P, Grau JB. Ectopic origin of left coronary ostium from left ventricle, with occlusive membrane. Tex Heart Inst J 2008;35:162-5.

13. Pinede L, Duhaut P, Loire R. Clinical presentation of left atrial cardiac myxoma. A series of 112 consecutive cases. Medicine (Baltimore) 2001;80:159-72.

14. Sykes KT, Gordon SG, Saunders AB, Vitt JP, O'Brien MT, Fries RC. Palliative combined cutting and high-pressure balloon valvuloplasty in six dogs with severe, symptomatic subaortic stenosis. J Vet Cardiol 2020;31:36-50.